 CMC, vol.6, no.1, pp.1-11, 2007

Characteristic of Waves in A Multi-Walled Carbon Nanotube

G. Q. Xie[1,2,3], X. Han[2] and S. Y. Long[3]

Abstract: A multi-walled carbon nanotube is modeled as a multiple-elastic cylindrical structure. The numerical-analytical method is adopted to analyze the characteristics of harmonic waves propagating along an anisotropic carbon nanotube. Each wall of the carbon nanotube is divided into three-nodal-line layer elements. The deflections of two adjacent tubes are coupled through the van der Waals. The governing equation of element is obtained from Hamilton's principle. A set of system equation of dynamics equilibrium for the entire structure is obtained by the assembling of all the elements. From solution of the eigenvalue equations, the dispersive characteristics, group velocities of multi-walled carbon nanotubes are achieved, and these properties of the six characteristic wave surfaces are also obtained.

Keyword: Multi-walled carbon nanotube; elastic wave; group velocity; dispersion; characteristic surfaces

1 Introduction

Carbon nanotubes have been demonstrated to possess dramatic mechanical and electronic properties such as high stiffness-to-weight and strength-to-weight ratios and excellent electrical and thermal conductivities (Treacy et al. 1996; Parnes et al. 2002; Li et al. 2003, etc). Due to their excellent physical, chemical, mechanical properties, carbon nanotubes have be used as structural elements in nanoscale devices or potential reinforcements in nanocomposite materials. To take advantage of the potential applications of carbon nanotubes, it is necessary to have the fundamental understanding of them. A lot of theoretical and experimental investigations have been carried out (e.g. Dai et al. 1998; Govindjee et al. 1999; Qian et al. 2002).

The theoretical methods adopted to investigate the mechanics properties of carbon nanotubes are roughly classified into two kinds, one kind is the molecular dynamics and the other is the continuum mechanics methods. Continuum beam or shell models can be used to analyze the static or dynamic mechanical properties of carbon nanotubes. Yoon et al. (2002), Zhang et al. (2005) have made use of continuum elastic beam models to study vibrations of the carbon nanotube. The single-Euler-beam model was employed to investigate wave propagation in multi-walled carbon nanotubes (e.g. Treacy et al. 1996; Poncharal et al. 1999; Popov et al. 2003). Yoon et al. (2002, 2003a, 2003b) pointed out that non-coaxial intertube vibration and transverse waves of multi-wall carbon nanotubes (MWNTs) will be excited with high frequencies, which would have substantial effects on both the natural frequencies and the wave speed of MWNTs. Recently, Wang and Varadan (2006) investigated wave characteristics of carbon nanotubes, they proposed the material properties from the discrete atomic nature of carbon nanotubes, compared the wave solution in a single-walled carbon nanotube by Euler-Bernoulli beam model and Timoshenko beam model, respectively. They also used Timoshenko beam model to study the wave propagation in a double walled carbon nanotube via a simple single beam theory by assuming coaxial motion of the two tubes, and a double beam theory accounting for van der Waals. Chakraborty et al. (2006) used

[1] College of Civil Engineering, Hunan university of science and technology, Xiangtan, 411201, P. R. China

[2] Corresponding author, email: hanxu@hnu.cn, Fax: 86-731-8822051. State Key Laboratory of Advanced Design and Manufacturing for Vehicle Body, Hunan University, Changsha 410082, P. R. China

[3] Department of Engineering Mechanics, Hunan University, Changsha 410082, P. R. China

a spectrally formulated finite element to study elastic waves in CNTs. They investigated the effect of the number of walls on the frequency response function, and analyzed the response of multi-walled carbon nanotubes for terahertz level loading. Xie and Long (2006) investigated vibration behavior of a carbon nanotube based on micropolar elasticity.

Xi et al. (2000) use numerical-analytical method to investigate dispersion and characteristic surfaces of waves of laminated composite circular cylindrical shells, and Han et al. (2004) adopted this method to analyze transient response in cross-ply laminated cylinders and its application to reconstruction of elastic constants. In this paper, the numerical-analytical method is adopted to investigate the characteristics of wave propagating along a carbon nanotube. The multi-walled carbon nanotube is first divide into annular elements, the quadratic radial interpolate function is used for the shape function of the element in the radial direction. With the help of the solution of the eigenvalue equations, the group velocity, dispersion curve and the six characteristic surfaces of the waves in multi-walled carbon nanotubes are obtained. Numerical results have been presented to illustrate the characteristics of waves in nanotubes.

2 Formulations

Fig. 1 shows a N-walled carbon nanotube with the inner, outer radius and the thickness R_I, R_O and H, respectively. The material constants of grapheme is (Liu and Zheng, 2002)

$$\mathbf{D} = 1e^9 \begin{bmatrix} 1060 & 180 & 15 & 0 & 0 & 0 \\ & 1060 & 15 & 0 & 0 & 0 \\ & & 36.5 & 0 & 0 & 0 \\ & & & 4.5 & 0 & 0 \\ \text{sym} & & & & 4.5 & 0 \\ & & & & & 440 \end{bmatrix} \text{p}_a \tag{1}$$

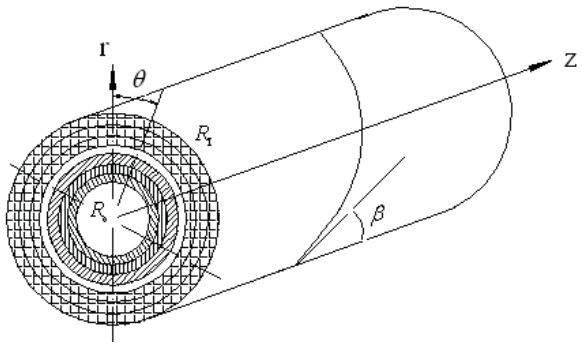

Figure 1: The shell model of carbon nanotube

2.1 Basic equation

The strain and stress relation of carbon nanotube is given by

$$\boldsymbol{\sigma} = \mathbf{D}\boldsymbol{\varepsilon} \tag{2}$$

where $\boldsymbol{\sigma} = [\sigma_z, \sigma_\theta, \sigma_r, \sigma_{\theta r}, \sigma_{rz}, \sigma_{z\theta}]^{\mathrm{T}}$ and $\boldsymbol{\varepsilon} = [\varepsilon_z, \varepsilon_\theta, \varepsilon_r, \varepsilon_{\theta r}, \varepsilon_{rz}, \varepsilon_{z\theta}]^{\mathrm{T}}$ are the vectors of the stresses and strains, respectively.

The geometric equations are written in matrix form

$$\boldsymbol{\varepsilon} = \mathbf{L}\mathbf{u} \tag{3}$$

where

$$\mathbf{L} = \begin{bmatrix} \frac{\partial}{\partial z} & 0 & 0 & 0 & \frac{\partial}{\partial r} & \frac{1}{r}\frac{\partial}{\partial \theta} \\ 0 & \frac{1}{r}\frac{\partial}{\partial \theta} & 0 & \frac{\partial}{\partial r} - \frac{1}{r} & 0 & \frac{\partial}{\partial z} \\ 0 & \frac{1}{r} & \frac{\partial}{\partial r} & \frac{1}{r}\frac{\partial}{\partial \theta} & \frac{\partial}{\partial z} & 0 \end{bmatrix}^{\mathrm{T}},$$

$$\mathbf{u} = \{u, v, w\}^{\mathrm{T}}$$

where u, v, w are the displacements in the axial, circumferential and radial directions, respectively.

The matrix $\mathbf{L}$ can be expressed as

$$\mathbf{L} = L_1\frac{\partial}{\partial z} + L_2\frac{\partial}{r\partial \theta} + L_3\frac{\partial}{\partial r} + L_4\frac{1}{r} \tag{4}$$

where L_1, L_2, L_3 and L_4 can be inspected from eq. (4).

2.2 Van der Waals pressure

Multi-walled carbon nanotubes possess hollow multilayer structure which interacts with the adjacent tubes by van der Waals forces. The net van

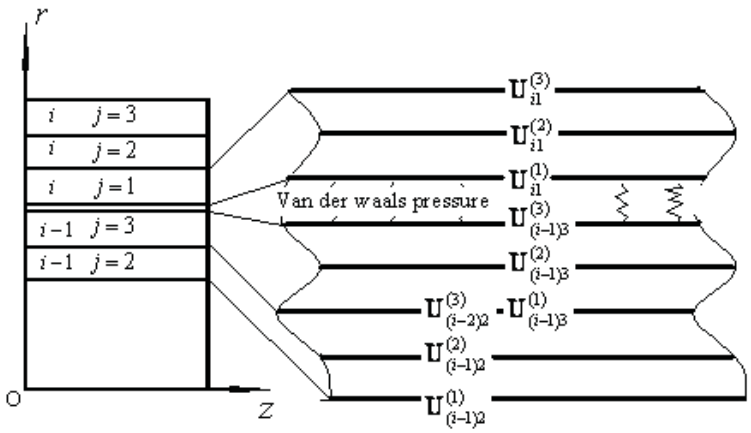

Figure 2: Annular element subdivision and the isolated annular element

der Waals pressure at any point between adjacent tubes is a linear function of the difference of deflection at that point. The pressure $p_{i(i+1)}$ on tube i due to tube $i+1$ is (Yoon et al. (2003b))

$$p_{i(i+1)} = \varsigma_i (w_{i+1} - w_i) \quad (i = 1, 2, \ldots, N) \tag{5}$$

where, the subscripts i, $i+1$ represents the numbers of the two adjacent tubes, respectively, w_i is the inward deflection of tube i, and the van der Waals interaction coefficient ς_i is given by Yoon et al. (2003b)

$$\varsigma_i = \frac{320(2R_i)\text{erg/cm}^2}{0.16d^2} \tag{6}$$

where $d = 0.142$nm, R_i is the inner radius of tube i.

From Eqs. (6) and (7), the following relation between $p_{(i+1)i}$ and $p_{i(i+1)}$ can be obtained.

$$p_{(i+1)i} = -\frac{R_i}{R_{i+1}} p_{i(i+1)} \tag{7}$$

2.3 Dispersive equation

We use annular elements to model the radial displacement component of the carbon nanotube, while the axial and circumferential displacement components are dealt with analytically. Every wall is divided into three annular elements. The subdivision of an annular element and the relations of the adjacent element are shown in Fig. 2. Each element has the inner, middle, and outer nodal surfaces donated by $1, 2, 3$.

The displacement field within the jth element of the ith tube can be approximated as

$$\mathbf{u}_{ij} = \mathbf{N}(r)\mathbf{U}_{ij} \tag{8}$$

where the matrix of shape function of the jth element of the ith tube

$$N(r) = \left[\left(1 - 3\overline{r} + 2\overline{r}^2\right)\mathbf{I} \;\; 4\left(\overline{r} - \overline{r}^2\right)\mathbf{I} \;\; \left(-\overline{r} + 2\overline{r}^2\right)\mathbf{I}\right]$$

where $\mathbf{I}$ is a 3×3 identity matrix and $\overline{r} = (r - r_{ij}) / \left(r_{i(j+1)} - r_{ij}\right)$. r_{ij} is the inner radius of the jth element of the ith tube. The vector of the nodal surface displacement amplitudes of the element of the jth element of the ith tube is written as

$$\mathbf{U}_{ij} = \left[U_{ij}^{(1)}\; V_{ij}^{(1)}\; W_{ij}^{(1)}\; U_{ij}^{(2)}\; V_{ij}^{(2)}\; W_{ij}^{(2)}\; U_{ij}^{(3)}\; V_{ij}^{(3)}\; W_{ij}^{(3)}\right]^{\mathrm{T}} \tag{9}$$

The governing equation of the element could be developed by means of the Hamilton variational principle, which takes the form

$$\int_{t_0}^{t_1} \delta\left(P_{ij} - T_{ij}\right)\mathrm{d}t = 0 \tag{10}$$

Here, the time t_0 and t_1 are arbitrary, P_{ij} and T_{ij} are the potential energy and kinetic energy of the jth element of the ith tube, respectively.

The potential energy in the absence of body force is given by

$$P_{ij}=\frac{1}{2}\int_{-\infty}^{+\infty}\int_{0}^{2\pi}\int_{r_{ij}}^{r_{i(j+1)}}\boldsymbol{\varepsilon}_{ij}^{\mathrm{T}}\boldsymbol{\sigma}_{ij}r\mathrm{d}r\mathrm{d}\theta\mathrm{d}z$$
$$j=2,\ i=1,\ldots,N \text{ or } j=1,\ i=1 \text{ or } j=3,\ i=N \tag{11a}$$

$$P_{ij}=\frac{1}{2}\int_{-\infty}^{+\infty}\int_{0}^{2\pi}\int_{r_{ij}}^{r_{i(j+1)}}\boldsymbol{\varepsilon}_{ij}^{\mathrm{T}}\boldsymbol{\sigma}_{ij}r\mathrm{d}r\mathrm{d}\theta\mathrm{d}z - \int_{-\infty}^{+\infty}\int_{r_{ij}}^{r_{i(j+1)}}p_{i(i+1)}\left(\mathbf{n}\frac{\partial\mathbf{u}_{ij}}{\partial r}\right)\mathrm{d}r\mathrm{d}z$$
$$j=3,\ i=1,2,\ldots,N-1 \tag{11b}$$

$$P_{ij}=\frac{1}{2}\int_{-\infty}^{+\infty}\int_{0}^{2\pi}\int_{r_{ij}}^{r_{i(j+1)}}\boldsymbol{\varepsilon}_{ij}^{\mathrm{T}}\boldsymbol{\sigma}_{ij}r\mathrm{d}r\mathrm{d}\theta\mathrm{d}z - \int_{-\infty}^{+\infty}\int_{r_{ij}}^{r_{i(j+1)}}p_{i(i+1)}\left(\mathbf{n}\frac{\partial\mathbf{u}_{ij}}{\partial r}\right)\mathrm{d}r\mathrm{d}z$$
$$j=1,\ i=2,3,\ldots,N \tag{11c}$$

where $\mathbf{n}=\{0,0,1\}$.

Substituting Eqs. (8) and (9) into Eq. (11), in view of Eqs. (1) and (5), gives

$$\begin{aligned}P_{ij}=\frac{1}{2}\int_{-\infty}^{+\infty}\int_{0}^{2\pi}\int_{r_{ij}}^{r_{i(j+1)}}&\left(\frac{\partial\mathbf{u}_{ij}^{\mathrm{T}}}{\partial z}\mathbf{c}_{11}\frac{\partial\mathbf{u}_{ij}}{\partial z}+\frac{\partial\mathbf{u}_{ij}^{\mathrm{T}}}{\partial z}\mathbf{c}_{12}\frac{1}{r}\frac{\partial\mathbf{u}_{ij}}{\partial\theta}+\frac{\partial\mathbf{u}_{ij}^{\mathrm{T}}}{\partial z}\mathbf{c}_{13}\frac{\partial\mathbf{u}_{ij}}{\partial r}\right.\\&+\frac{1}{r}\frac{\partial\mathbf{u}_{ij}^{\mathrm{T}}}{\partial z}\mathbf{c}_{14}\mathbf{u}_{ij}+\frac{1}{r}\frac{\partial\mathbf{u}_{ij}^{\mathrm{T}}}{\partial\theta}\mathbf{c}_{12}^{\mathrm{T}}\frac{\partial\mathbf{u}_{ij}}{\partial z}+\frac{1}{r^2}\frac{\partial\mathbf{u}_{ij}^{\mathrm{T}}}{\partial\theta}\mathbf{c}_{22}\frac{\partial\mathbf{u}_{ij}}{\partial\theta}\\&+\frac{1}{r}\frac{\partial\mathbf{u}_{ij}^{\mathrm{T}}}{\partial\theta}\mathbf{c}_{23}\frac{\partial\mathbf{u}_{ij}}{\partial r}+\frac{1}{r^2}\frac{\partial\mathbf{u}_{ij}^{\mathrm{T}}}{\partial\theta}\mathbf{c}_{24}\mathbf{u}_{ij}+\frac{\partial\mathbf{u}_{ij}^{\mathrm{T}}}{\partial r}\mathbf{c}_{13}^{\mathrm{T}}\frac{\partial\mathbf{u}_{ij}}{\partial z}\\&+\frac{1}{r}\frac{\partial\mathbf{u}_{ij}^{\mathrm{T}}}{\partial r}\mathbf{c}_{23}^{\mathrm{T}}\frac{\partial\mathbf{u}_{ij}}{\partial\theta}+\frac{\partial\mathbf{u}_{ij}^{\mathrm{T}}}{\partial r}\mathbf{c}_{33}\frac{\partial\mathbf{u}_{ij}}{\partial r}+\frac{1}{r}\frac{\partial\mathbf{u}_{ij}^{\mathrm{T}}}{\partial r}\mathbf{c}_{34}\mathbf{u}_{ij}\\&+\frac{1}{r}\mathbf{u}_{ij}^{\mathrm{T}}\mathbf{c}_{14}^{\mathrm{T}}\frac{\partial\mathbf{u}_{ij}}{\partial z}+\frac{1}{r^2}\mathbf{u}_{ij}\mathbf{c}_{24}^{\mathrm{T}}\frac{\partial\mathbf{u}_{ij}}{\partial\theta}+\frac{1}{r}\mathbf{u}_{ij}^{\mathrm{T}}\mathbf{c}_{34}^{\mathrm{T}}\frac{\partial\mathbf{u}_{ij}}{\partial r}\\&\left.+\frac{1}{r^2}\mathbf{u}_{ij}\mathbf{c}_{44}^{\mathrm{T}}\mathbf{u}_{ij}\right)\mathrm{d}r\mathrm{d}\theta\mathrm{d}z\end{aligned} \tag{12a}$$

where $(j=2,\ i=1,2,\ldots,N)$ or $(j=1,\ i=1)$ or $(j=3, i=N)$

$$\begin{aligned}P_{ij}=\frac{1}{2}\int_{0}^{2\pi}\int_{-\infty}^{+\infty}\int_{r_{ij}}^{r_{i(j+1)}}&\left(\frac{\partial\mathbf{u}_{ij}^{\mathrm{T}}}{\partial z}\mathbf{c}_{11}\frac{\partial\mathbf{u}_{ij}}{\partial z}+\frac{\partial\mathbf{u}_{ij}^{\mathrm{T}}}{\partial z}\mathbf{c}_{12}\frac{1}{r}\frac{\partial\mathbf{u}_{ij}}{\partial\theta}+\frac{\partial\mathbf{u}_{ij}^{\mathrm{T}}}{\partial z}\mathbf{c}_{13}\frac{\partial\mathbf{u}_{ij}}{\partial r}\right.\\&+\frac{1}{r}\frac{\partial\mathbf{u}_{ij}^{\mathrm{T}}}{\partial z}\mathbf{c}_{14}\mathbf{u}_{ij}+\frac{1}{r}\frac{\partial\mathbf{u}_{ij}^{\mathrm{T}}}{\partial\theta}\mathbf{c}_{12}^{\mathrm{T}}\frac{\partial\mathbf{u}_{ij}}{\partial z}+\frac{1}{r^2}\frac{\partial\mathbf{u}_{ij}^{\mathrm{T}}}{\partial\theta}\mathbf{c}_{22}\frac{\partial\mathbf{u}_{ij}}{\partial\theta}\\&+\frac{1}{r}\frac{\partial\mathbf{u}_{ij}^{\mathrm{T}}}{\partial\theta}\mathbf{c}_{23}\frac{\partial\mathbf{u}_{ij}}{\partial r}+\frac{1}{r^2}\frac{\partial\mathbf{u}_{ij}^{\mathrm{T}}}{\partial\theta}\mathbf{c}_{24}\mathbf{u}_{ij}+\frac{\partial\mathbf{u}_{ij}^{\mathrm{T}}}{\partial r}\mathbf{c}_{13}^{\mathrm{T}}\frac{\partial\mathbf{u}_{ij}}{\partial z}\\&+\frac{1}{r}\frac{\partial\mathbf{u}_{ij}^{\mathrm{T}}}{\partial r}\mathbf{c}_{23}^{\mathrm{T}}\frac{\partial\mathbf{u}_{ij}}{\partial\theta}+\frac{\partial\mathbf{u}_{ij}^{\mathrm{T}}}{\partial r}\mathbf{c}_{33}\frac{\partial\mathbf{u}_{ij}}{\partial r}+\frac{1}{r}\frac{\partial\mathbf{u}_{ij}^{\mathrm{T}}}{\partial r}\mathbf{c}_{34}\mathbf{u}_{ij}\\&+\frac{1}{r}\mathbf{u}_{ij}^{\mathrm{T}}\mathbf{c}_{14}^{\mathrm{T}}\frac{\partial\mathbf{u}_{ij}}{\partial z}+\frac{1}{r^2}\mathbf{u}_{ij}\mathbf{c}_{24}^{\mathrm{T}}\frac{\partial\mathbf{u}_{ij}}{\partial\theta}+\frac{1}{r}\mathbf{u}_{ij}^{\mathrm{T}}\mathbf{c}_{34}^{\mathrm{T}}\frac{\partial\mathbf{u}_{ij}}{\partial r}\\&\left.+\frac{1}{r^2}\mathbf{u}_{ij}\mathbf{c}_{44}^{\mathrm{T}}\mathbf{u}_{ij}\right)\mathrm{d}r\mathrm{d}z\mathrm{d}\theta\\&-\int_{-\infty}^{+\infty}\int_{r_{ij}}^{r_{i(j+1)}}\varsigma_i\left(\mathbf{u}_{ij}^{\mathrm{T}}\mathbf{n}^{\mathrm{T}}\right)\left(\mathbf{n}\frac{\partial\mathbf{u}_{ij}}{\partial r}\right)\mathrm{d}r\mathrm{d}z\\&+\int_{-\infty}^{+\infty}\int_{r_{ij}}^{r_{i(j+1)}}\varsigma_i\left(\mathbf{u}_{(i+1)(j-2)}^{\mathrm{T}}\mathbf{n}^{\mathrm{T}}\right)\left(\mathbf{n}\frac{\partial\mathbf{u}_{ij}}{\partial r}\right)\mathrm{d}r\mathrm{d}z\end{aligned} \tag{12b}$$

where $j=3,\ i=1,2,\ldots,N-1$

$$\begin{aligned}P_{ij}=\int_{0}^{2\pi}\int_{-\infty}^{+\infty}\int_{r_{ij}}^{r_{i(j+1)}}&\left(\frac{\partial\mathbf{u}_{ij}^{\mathrm{T}}}{\partial z}\mathbf{c}_{11}\frac{\partial\mathbf{u}_{ij}}{\partial z}+\frac{\partial\mathbf{u}_{ij}^{\mathrm{T}}}{\partial z}\mathbf{c}_{12}\frac{1}{r}\frac{\partial\mathbf{u}_{ij}}{\partial\theta}+\frac{\partial\mathbf{u}_{ij}^{\mathrm{T}}}{\partial z}\mathbf{c}_{13}\frac{\partial\mathbf{u}_{ij}}{\partial r}\right.\\&+\frac{1}{r}\frac{\partial\mathbf{u}_{ij}^{\mathrm{T}}}{\partial z}\mathbf{c}_{14}\mathbf{u}_{ij}+\frac{1}{r}\frac{\partial\mathbf{u}_{ij}^{\mathrm{T}}}{\partial\theta}\mathbf{c}_{12}^{\mathrm{T}}\frac{\partial\mathbf{u}_{ij}}{\partial z}+\frac{1}{r^2}\frac{\partial\mathbf{u}_{ij}^{\mathrm{T}}}{\partial\theta}\mathbf{c}_{22}\frac{\partial\mathbf{u}_{ij}}{\partial\theta}\\&+\frac{1}{r}\frac{\partial\mathbf{u}_{ij}^{\mathrm{T}}}{\partial\theta}\mathbf{c}_{23}\frac{\partial\mathbf{u}_{ij}}{\partial r}+\frac{1}{r^2}\frac{\partial\mathbf{u}_{ij}^{\mathrm{T}}}{\partial\theta}\mathbf{c}_{24}\mathbf{u}_{ij}+\frac{\partial\mathbf{u}_{ij}^{\mathrm{T}}}{\partial r}\mathbf{c}_{13}^{\mathrm{T}}\frac{\partial\mathbf{u}_{ij}}{\partial z}\\&+\frac{1}{r}\frac{\partial\mathbf{u}_{ij}^{\mathrm{T}}}{\partial r}\mathbf{c}_{23}^{\mathrm{T}}\frac{\partial\mathbf{u}_{ij}}{\partial\theta}+\frac{\partial\mathbf{u}_{ij}^{\mathrm{T}}}{\partial r}\mathbf{c}_{33}\frac{\partial\mathbf{u}_{ij}}{\partial r}+\frac{1}{r}\frac{\partial\mathbf{u}_{ij}^{\mathrm{T}}}{\partial r}\mathbf{c}_{34}\mathbf{u}_{ij}\\&+\frac{1}{r}\mathbf{u}_{ij}^{\mathrm{T}}\mathbf{c}_{14}^{\mathrm{T}}\frac{\partial\mathbf{u}_{ij}}{\partial z}+\frac{1}{r^2}\mathbf{u}_{ij}\mathbf{c}_{24}^{\mathrm{T}}\frac{\partial\mathbf{u}_{ij}}{\partial\theta}+\frac{1}{r}\mathbf{u}_{ij}^{\mathrm{T}}\mathbf{c}_{34}^{\mathrm{T}}\frac{\partial\mathbf{u}_{ij}}{\partial r}\\&\left.+\frac{1}{r^2}\mathbf{u}_{ij}\mathbf{c}_{44}^{\mathrm{T}}\mathbf{u}_{ij}\right)\mathrm{d}r\mathrm{d}z\mathrm{d}\theta\\&-\int_{-\infty}^{+\infty}\int_{r_{ij}}^{r_{i(j+1)}}\varsigma_i\left(\mathbf{u}_{ij}^{\mathrm{T}}\mathbf{n}^{\mathrm{T}}\right)\left(\mathbf{n}\frac{\partial\mathbf{u}_{ij}}{\partial r}\right)\mathrm{d}r\mathrm{d}z\\&+\int_{-\infty}^{+\infty}\int_{r_{ij}}^{r_{i(j+1)}}\varsigma_i\left(\mathbf{u}_{(i-1)(j+2)}^{\mathrm{T}}\mathbf{n}^{\mathrm{T}}\right)\left(\mathbf{n}\frac{\partial\mathbf{u}_{ij}}{\partial r}\right)\mathrm{d}r\mathrm{d}z\end{aligned} \tag{12c}$$

where $j = 1\ i = 2,3,\ldots,N$.

$$\mathbf{c}_{ij} = \mathbf{L}_i^{\mathrm{T}}\mathbf{D}\mathbf{L}_j \quad i,j = 1,2,3,4 \tag{13}$$

The kinetic energy of the element is expressed in terms of the displacement vector as

$$T_{ij} = \frac{1}{2}\int_{-\infty}^{+\infty}\int_{0}^{2\pi}\int_{r_{ij}}^{r_{i(j+1)}} \frac{\partial \mathbf{u}_{ij}^{\mathrm{T}}}{\partial t}\frac{\partial \mathbf{u}_{ij}}{\partial t}\rho r\mathrm{d}r\mathrm{d}\theta\mathrm{d}z \tag{14}$$

Substituting Eqs. (12) and (14) into Eq. (10), and taking variation with respect to $\mathbf{U}$ leads to the following governing differential equations of the element

$$\mathbf{M}^e\ddot{\mathbf{U}}^e + \mathbf{K}_D^e\mathbf{U}^e = \mathbf{q}^e \tag{15}$$

Where the dot represents the derivative with respect to the time, the superscript 'e' denotes element and

$$\mathbf{K}_D^e = -\mathbf{A}_6^e\frac{\partial^2}{\partial z^2} - \mathbf{A}_5^e\frac{\partial^2}{\partial\theta\partial z} - \mathbf{A}_4^e\frac{\partial^2}{\partial\theta 2} + \mathbf{A}_3^e\frac{\partial}{\partial z} + \mathbf{A}_2^e\frac{\partial}{\partial\theta} + \mathbf{A}_1^e \tag{16}$$

where $\mathbf{A}_l^e$ $(l = 1,2,\ldots,6)$ and $\mathbf{q}^e$ are expressed in the appendix.

The assembling of all the elements can get the total system differential equations for the whole nanotubes:

$$\mathbf{M}^t\ddot{\mathbf{U}}^t + \mathbf{K}_D^t\mathbf{U}^t = \mathbf{0} \tag{17}$$

where

$$\mathbf{K}_D^t = -\mathbf{A}_6^t\frac{\partial^2}{\partial z^2} - \mathbf{A}_5^t\frac{\partial^2}{\partial\theta\partial z} - \mathbf{A}_4^t\frac{\partial^2}{\partial\theta 2} + \mathbf{A}_3^t\frac{\partial}{\partial z} + \mathbf{A}_2^t\frac{\partial}{\partial\theta} + \mathbf{A}_1^t + \mathbf{q}^t \tag{18}$$

the superscript 't' represents the total. It should be noted that $\mathbf{q}^e$ of Eq. (15) is the coupled displace terms of the adjacent walls and assembled into $\mathbf{q}^t$, and $\mathbf{q}^t$ is incorporated by $\mathbf{K}_D^t$.

The whole stiff matrix $\mathbf{K}^t$, mass matrix $\mathbf{M}^t$, and the displacement vector $\mathbf{V}^t$ can be obtained by assembling the corresponding matrices and vectors of adjacent elements, respectively. The size of $\mathbf{V}^t$ is $21N$, the size of the matrices $\mathbf{M}^t$ and $\mathbf{K}^t$ are both $21N\times 21N$.

During the process of assembling elements, the following interface conditions are applied:

$$\mathbf{u}_{i1}^{(3)} = \mathbf{u}_{i2}^{(1)}, \quad \mathbf{u}_{i2}^{(3)} = \mathbf{u}_{i3}^{(1)}, \quad p_{(i+1)i} = -\frac{R_i}{R_{i+1}}p_{i(i+1)} \tag{19}$$

It should be noted that $p_{i(i+1)}$ is the pressure on 3-th element of i-th tube due to $(i+1)$-th tube, and $p_{(i+1)i}$ is the van der waals pressure on 1-th element of $(i+1)$-th.

The displace vector $\mathbf{U}^t(\theta,z,t)$ of the element is expressed as the complex exponentials

$$\mathbf{U}^t(\theta,z,t) = \mathbf{V}^t\exp\left[\left(R_o k\sin\beta\right)\theta + \left(k\cos\beta\right)z - \omega t\right]i \tag{20}$$

Where $i = \sqrt{-1}$, ω is the angular frequency, k is the wavenumber, β is the helical angle of wave propagation with respect to the z-axial.

Substituting Eq. (20) into Eq. (17), has

$$\left[\mathbf{K}^t - \omega 2\mathbf{M}^t\right]\mathbf{V}^t = \mathbf{0} \tag{21}$$

Where

$$\mathbf{K}^t = \mathbf{A}_6^t k^2\cos 2\beta + \mathbf{A}_5^t R_0 k^2\cos\beta\sin\beta + \mathbf{A}_4^t R_0^2 k^2\sin 2\beta + i\mathbf{A}_3^t k\cos\beta + i\mathbf{A}_2^t R_0 k\sin\beta + \mathbf{A}_1^t + \mathbf{q}^t \tag{22}$$

The eigenvalue equation corresponding to Eq. (21) is

$$\left[K^t - \omega 2M^t\right]\varphi^R = 0 \tag{23}$$

From Eq. (23), the eigenfrequencies ω_j $(j = 1,2,\ldots,21N)$ and the right eigenvectors φ^R can be obtained.

In Eq. (23) $\mathbf{M}^t$ is a symmetric matrix and $\mathbf{K}^t$ is a Hermitian matrix for a given real wave number. For the mth mode, the eigenfrequency can be obtained from the Rayleigh quotient

$$\omega_m^2 = \frac{\varphi_m^L\mathbf{K}^t\varphi_m^R}{\varphi_m^L\mathbf{M}^t\varphi_m^R} \tag{24}$$

Where φ_m^L and φ_m^R are the mth transposed left and right eigenvectors of Eq. (23).

2.4 Wave surfaces

Following, we will make use of the Rayleigh quotient concept and the conception of references (Liu et al. (1991); Liu and Xi (2001)) to express mathematically characteristic wave surfaces.

Group velocity represents the rate at which energy is transported. It is defined as (Achenbach 1973)

$$c_g = \frac{\mathrm{d}\omega}{\mathrm{d}k} \tag{25}$$

Combination of Eq. (24) and Eq. (25), the group velocity of the mth mode can be given by Lysmer et al. (1970)

$$c_{gm} = \frac{\varphi_m^L \mathbf{K}_k^t \varphi_m^R}{2\omega_m \varphi_m^L \mathbf{M}^t \varphi_m^R} \tag{26}$$

Where

$$\mathbf{K}_k^t = 2k\mathbf{A}_6^t \cos 2\beta + 2k\mathbf{A}_5^t \cos\beta \sin\beta + 2k\mathbf{A}_4^t \sin 2\beta + i\mathbf{A}_3^t \cos\beta + i\mathbf{A}_2^t \sin\beta \tag{27}$$

From Eq. (26), the group velocity surface for the mth mode can be obtained

$$f_g(c_{gm}, \theta) = \varphi_m^L \mathbf{k}_k^t \varphi_m^R - 2c_{gm}\omega_m \varphi_m^L \mathbf{M}^t \varphi_m^R \tag{28}$$

The group slowness q_m for the mth mode is the reciprocal of the group velocity. The group slowness surface (GSS) shows the dependence of the relative arrival time of the energy of a plane wave on the direction of wave propagation. In the same way, the group slowness surface for the mth mode can be obtained

$$f_q(q_m, \theta) = q_m \varphi_m^L \mathbf{k}_k^t \varphi_m^R - 2\omega_m \varphi_m^L \mathbf{M}^t \varphi_m^R \tag{29}$$

Similarly, phase velocity surface and phase slowness surface, as well as group wave surface and phase wave surface can be obtained following the same way.

3 Results and discussions

The computational procedure is: Each wall of tube is divided into three annular elements of uniform thickness, an N-walled nanotubes possesses $3N$ elements. Based on the Hamilton's principle, the governing equations of each element are derived. The mass matrix $\mathbf{M}^t$ and stiff matrix $\mathbf{K}^t$ can be obtained by assembling the adjacent elements. The eigenvalues and eigenvectors of the system can be obtained by solving of eigenvalue equation (23) for various wavenumber k. Finally, the dispersive curves and group velocity of various modes can be obtained by using Eqs. (24) and (26), respectively.

The numerical examples are presented for dispersion and characteristic surfaces of harmonic helical waves in a carbon nanotube. The following dimensionless parameters are adopted:

$$\overline{c}_{ij} = c_{ij}/c_{44}, \quad \overline{k} = kH, \overline{R} = r/H, \quad \overline{\omega} = \omega H\sqrt{\rho_c/c_{44}} \tag{30}$$

where the reference properties c_{44} and ρ_c are the Young's modulus and the mass density of grapheme.

Fig. 3(a), (b) and (c) show that the dispersion curves of the waves propagating along the axial ($\beta = 0^o$), helical ($\beta = 30^o$) and circumferential ($\beta = 90^o$) direction of a 2-wall carbon nanotube with the inner radius 2nm, respectively. It can be observed from these figures that none of these dispersion curves pass through the coordination origin. This reveals that the group velocities aren't equal to the phase velocities; the waves for the carbon nanotube are dispersive. It can be observed from Figs. 3(a), (b) and (c) that the dispersion curves of the harmonic helical waves in the 2-wall carbon nanotube will changed with variation of the propagation direction of the waves.

The dispersions of the waves for two carbon nanotubes with similar wall number but different inner radii are shown by Fig. 4(a). It can be observed from Fig. 4(a) that the inner radius of the carbon nanotube influence less on the dispersive curve of these waves for smaller wavenumber, and that the larger the wavenumber, the stronger this effect.

Fig. 4(b) shows that the dispersive curves of the waves for two carbon nanotubes with similar inner radii but different wall number. It can be observed from Fig. 4(b) that the dispersive curves of the waves are influenced by the number of the wall of the carbon nanotube, the dispersive curves of the more wall carbon nanotube are below that

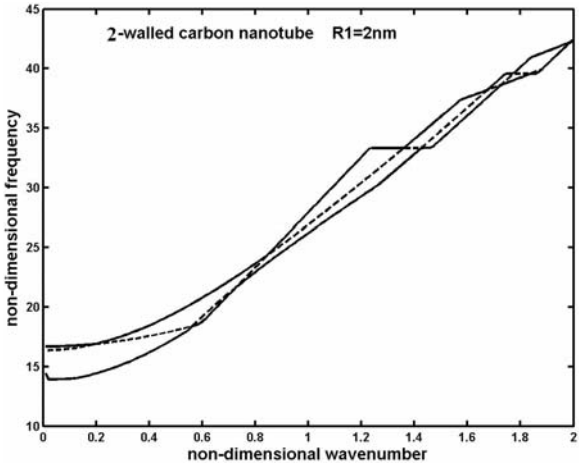

(a) $\beta = 0^o$

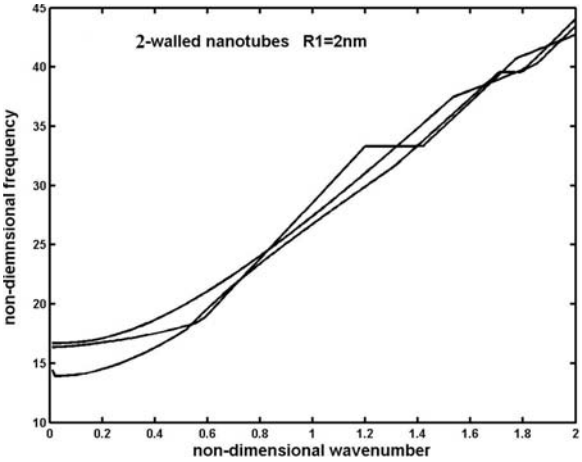

(b) $\beta = 30^o$

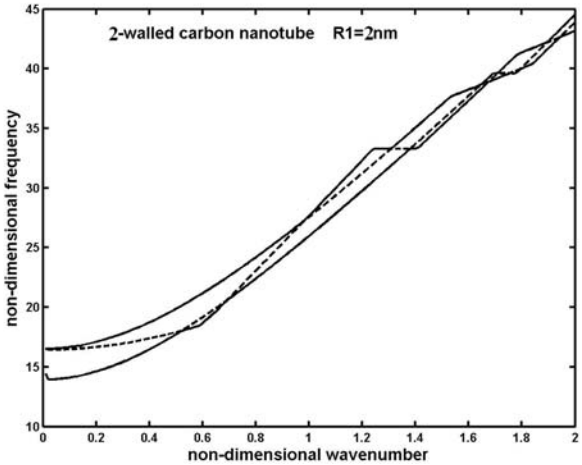

(c) $\beta = 90^o$

Figure 3: The dispersive curves of a 2-wall carbon nanotube

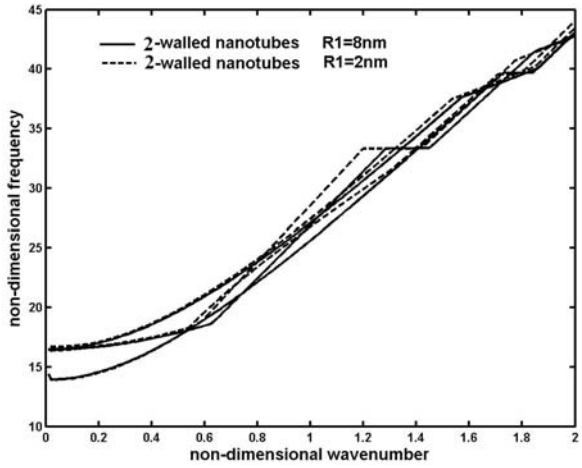

(a)

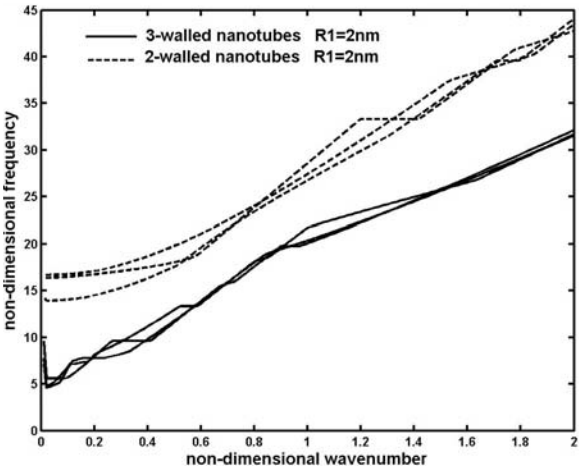

(b)

Figure 4: The dispersive curves of two carbon nanotubes $\beta = 30^o$

of the less wall ones. This can be explained as following. The numerical results show that the van der waals pressure is a less force, the connections of the adjacent walls of the multi-walled carbon nanotube can be regarded as the weak spring linking, the wall number more, the freedom number more, and the stiff of the system weaker, the frequency will decrease with the increasing of the wall number.

Figs. 5(a), (b) and (c) are the group velocity spectra of the waves for carbon nanotubes with their radii 2nm. The propagation directions of waves are chosen as$\beta = 0^o$, 30^o and 90^o, respectively. Figs. 5 indicate that the group velocity spectra are

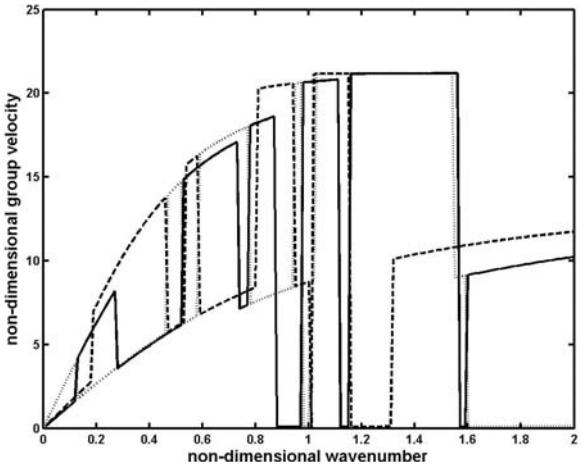

(a) $\beta = 0^o$ R_1=2nm

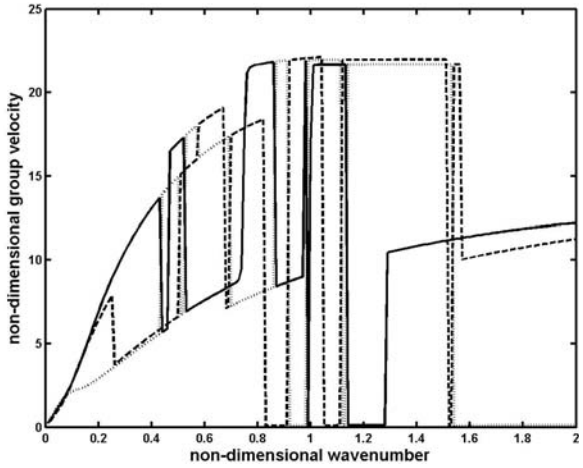

(b) $\beta = 30^o$ R_1=2nm

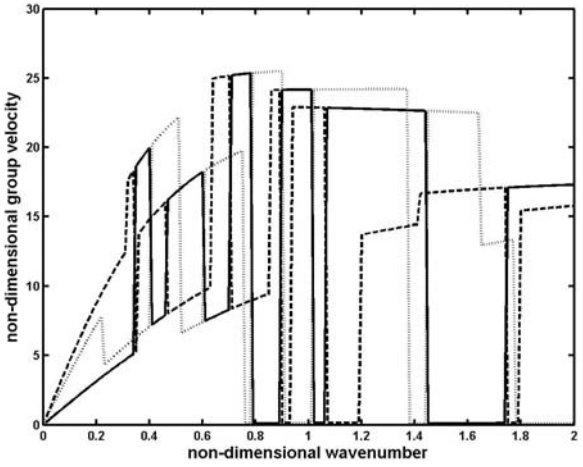

(c) $\beta = 90^o$ R_1=2nm

Figure 5: The group velocity curves of a 2-walled carbon nanotube

horizontal line at a small range of wavenumbers, this implies that the energy travels at a constant speed within these range of wavenumbers. The sudden jumps in the group velocities indicate the change of the order of the wave modes. It can be found from the comparison between Figs. 5(a), (b) and (c) that the group velocity will change as the direction of the wave propagating in the carbon nanotube varies.

It is observed from Fig. 6 that the group velocity spectra of waves for the carbon nanotube are influenced by the inner radius of the carbon nanotubes, the group velocity spectra for the carbon nanotube with the different inner radius are different.

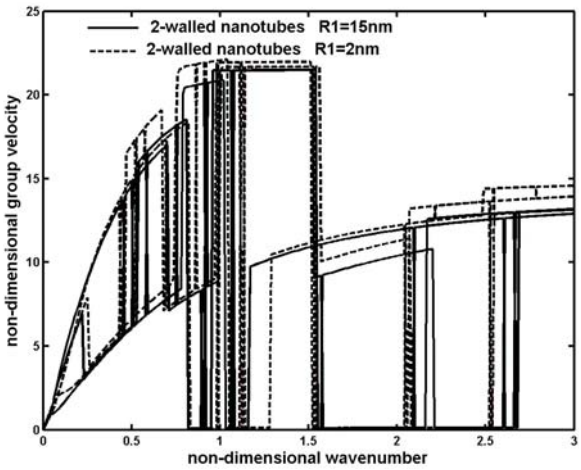

Figure 6: The group velocity curves of two carbon nanotubes $\beta = 30^o$

Figs. 7(a) and 7(b) illustrate six characteristic wave surfaces for the first two propagation modes of a 3-wall carbon nanotube ($R_1 = 2$nm). It can be found from these figures that none of wave surfaces of the first two modes are circular. This is the result that the elastic moduli of carbon nanotube are strongly anisotropic. From these figures, we can see very clearly that the wave propagation in the carbon nanotube depends strongly upon not only the wave propagation modes but also the anisotropy of the carbon nanotube material.

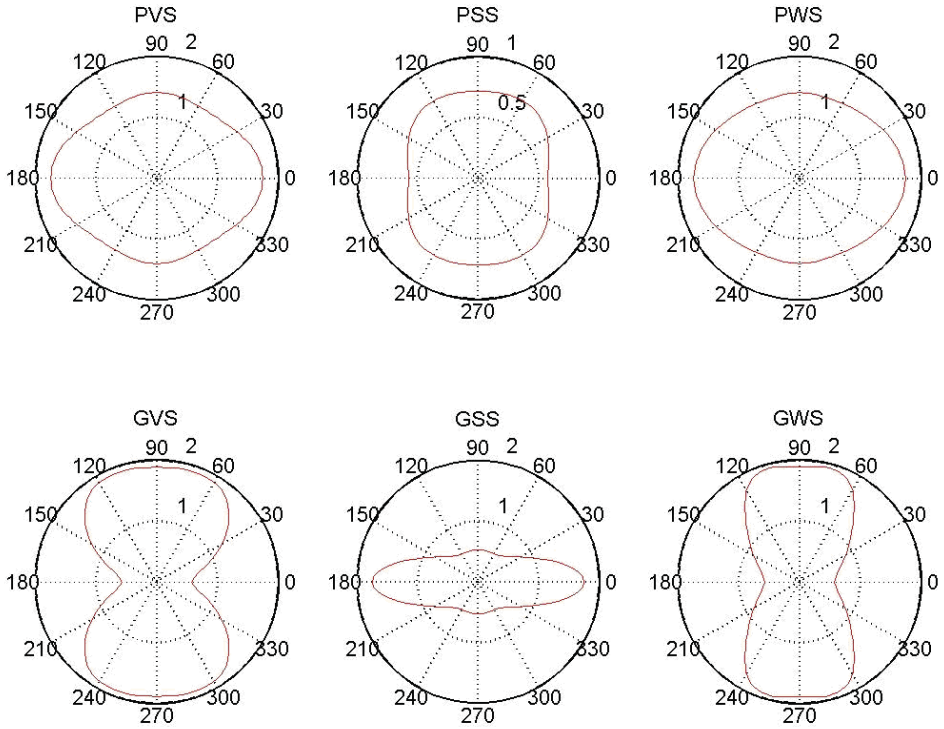

(a) First mode

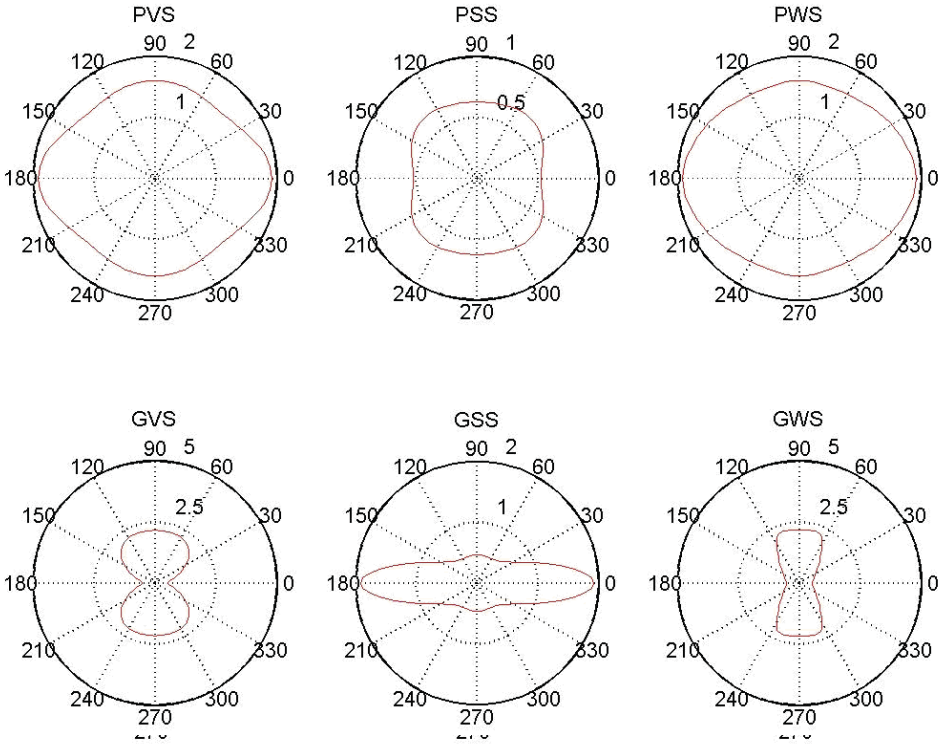

(b) Second mode

Figure 7: Characteristic wave surfaces for a 3-wall carbon nanotube (The innermost radius 2nm)

4 Conclusions

A multi-walled nanotube is modeled as a multiple-elastic cylindrical shell, and the deflections of all nested tubes are coupled through the van der Walls interaction between any two adjacent tubes. The governing equations of each element are obtained from the Hamilton's. The dispersive curve of the waves can be obtained from the solution of the eigenvalue equations, the group velocity and six characteristic wave surfaces of the waves for the multi-walled carbon nanotubes can also be obtained. The numerical results show that the dispersion, the group velocity of carbon nanotubes are influenced by the number of wall, the innermost radius of carbon nanotubes and the direction of the waves propagating in the carbon nanotube.

Acknowledgement: This work is supported by the National Science Foundation of China under the grant number 10572048, the Hunan province Science Foundation under the grant number 06JJ1002 and CFC fund 9140C82040206KG0104.

Appendix

$$\mathbf{A}_6^e = \int_{r_{ij}}^{r_{i(j+1)}} \mathbf{N}^{\mathrm{T}} \mathbf{c}_{11} \mathbf{N} r \mathrm{d}r$$

$$\mathbf{A}_5^e = \int_{r_{ij}}^{r_{i(j+1)}} N^{\mathrm{T}} \left(\mathbf{c}_{12} + \mathbf{c}_{12}^{\mathrm{T}}\right) N \mathrm{d}r$$

$$\mathbf{A}_4^e = \int_{r_{ij}}^{r_{i(j+1)}} \frac{1}{r} N^{\mathrm{T}} \mathbf{c}_{22} N \mathrm{d}r$$

$$\mathbf{A}_3^e = \int_{r_{ij}}^{r_{i(j+1)}} \left(-\mathbf{N}^{\mathrm{T}} \mathbf{c}_{13} \frac{\partial \mathbf{N}}{\partial r} + \frac{\partial \mathbf{N}^{\mathrm{T}}}{\partial r} \mathbf{c}_{13}^{\mathrm{T}} \mathbf{N} + \frac{1}{r} \mathbf{N}^{\mathrm{T}} \left(\mathbf{c}_{14}^{\mathrm{T}} - \mathbf{c}_{14}\right) \mathbf{N} \right) r \mathrm{d}r$$

$$\mathbf{A}_2^e = \int_{r_{ij}}^{r_{i(j+1)}} \left(-\mathbf{N}^{\mathrm{T}} \mathbf{c}_{23} \frac{\partial \mathbf{N}}{\partial r} + \frac{\partial \mathbf{N}^{\mathrm{T}}}{\partial r} \mathbf{c}_{23}^{\mathrm{T}} \mathbf{N} + \frac{1}{r} \mathbf{N}^{\mathrm{T}} \left(\mathbf{c}_{24}^{\mathrm{T}} - \mathbf{c}_{24}\right) \mathbf{N} \right) \mathrm{d}r$$

$$\mathbf{A}_1^e = \int_{r_{ij}}^{r_{i(j+1)}} \left(\frac{\partial \mathbf{N}^{\mathrm{T}}}{\partial r} \mathbf{c}_{33} \frac{\partial \mathbf{N}}{\partial r} + \frac{1}{r} \frac{\partial \mathbf{N}^{\mathrm{T}}}{\partial r} \mathbf{c}_{34} \mathbf{N} + \frac{1}{r^2} \mathbf{N}^{\mathrm{T}} \mathbf{c}_{44} \mathbf{N} + \frac{1}{r} \mathbf{N}^{\mathrm{T}} \mathbf{c}_{34}^{\mathrm{T}} \frac{\partial \mathbf{N}}{\partial r} \right) r \mathrm{d}r$$

$$\mathbf{M}^e = \int_{r_{ij}}^{r_{i(j+1)}} \mathbf{N}^{\mathrm{T}} \mathbf{N} \rho r \mathrm{d}r$$

The terms of the van der Waals are given by

(1) $j = 2,\ i = 1, 2, \ldots, N$ or $j = 1,\ i = 1$

$$\mathbf{q}_{ij} = \mathbf{0}$$

(2) $j = 3,\ i = 1, 2, \ldots, N-1$

$$\mathbf{q}_{ij} = \frac{1}{2\pi} \left(\int_0^{h_{ij}} \varsigma_1 \left(\mathbf{N}_{ij}^{\mathrm{T}} \mathbf{n}^{\mathrm{T}}\right) \left(\mathbf{n} \frac{\partial \mathbf{N}_{ij}}{\partial r} \right) \mathrm{d}r \mathbf{U}_{ij} - \int_{r_{i-1}}^{r_i} \varsigma_1 \left(\mathbf{N}_{(i+1)(j-2)}^{\mathrm{T}} \mathbf{n}^{\mathrm{T}}\right) \left(\mathbf{n} \frac{\partial \mathbf{N}_{ij}}{\partial r} \right) \mathrm{d}r \cdot \mathbf{U}_{(i+1)(j-2)} \right)$$

where, $\mathbf{n} = \{0, 0, 1\}$

(3) $j = 1,\ i = 2, 3, \ldots, N$

$$\mathbf{q}_{ij} = \frac{1}{2\pi} \int_0^{h_{ij}} \left(\varsigma_j \left(\mathbf{N}_{ij}^{\mathrm{T}} \mathbf{n}^{\mathrm{T}}\right) \left(\mathbf{n} \frac{\partial \mathbf{N}_{ij}}{\partial r} \right) \mathbf{U}_{ij} - \int_0^h \varsigma_j \left(\mathbf{N}_{ij}^{\mathrm{T}} \mathbf{n}^{\mathrm{T}}\right) \left(\mathbf{n} \frac{\partial \mathbf{N}_{(i-1)(j+2)}}{\partial r} \right) \cdot \mathbf{U}_{(i-1)(j+2)} \mathrm{d}r \right)$$

$$\mathbf{B}_1 = \mathbf{A}_{lij} + \hat{\lambda}_j^N \left(S_j\right)$$

where $\hat{\lambda}_j^N$ is an assembling operator.

$$\mathbf{S}_j = \begin{bmatrix} \mathrm{M1} & \mathrm{M2} \\ \mathrm{M3} & \mathrm{M4} \end{bmatrix}$$

where

$$\mathrm{M1} = \frac{1}{2\pi} \int_0^h \varsigma_j \left(\frac{\partial \mathbf{N}_{ij}^{\mathrm{T}}}{\partial r} \mathbf{n}^{\mathrm{T}} \right) \left(\mathbf{n} \mathbf{N}_{ij} \right) \mathrm{d}r$$

$$\mathrm{M2} = -\frac{1}{2\pi} \int_0^h \varsigma_j \left(\frac{\partial \mathbf{N}_{ij}^{\mathrm{T}}}{\partial r} \mathbf{n}^{\mathrm{T}} \right) \left(\mathbf{n} \mathbf{N}_{i(j+1)} \right) \mathrm{d}r$$

$$\mathrm{M3} = -\frac{1}{2\pi} \int_0^h \varsigma_j \left(\frac{\partial \mathbf{N}_{ij}^{\mathrm{T}}}{\partial r} \mathbf{n}^{\mathrm{T}} \right) \left(\mathbf{n} \mathbf{N}_{i(j+1)} \right) \mathrm{d}r$$

$$\mathrm{M4} = \frac{1}{2\pi} \int_0^h \varsigma_{j+1} \left(\frac{\partial \mathbf{N}_{i(j+1)}^{\mathrm{T}}}{\partial r} \mathbf{n}^{\mathrm{T}} \right) \left(\mathbf{n} \mathbf{N}_{i(j+1)} \right) \mathrm{d}r$$

References

Achenbach, J. D. (1973): Wave Propagation in Elastic Solids, North-Holland, Amsterdam.

Chakraborty, A., SIvakumar, M. S., Gopalakrishnan, S. (2006): Spectral element based model for wave propagation analysis in multi-wall carbon nanotubes. *International Journal of Solids and Structures*. 43(2): 279-294.

Dai, H. J., Franklin, N. (1998): Exploiting the properties of carbon nanotubes for nanolithography. *Appl. Phys. Lett.*. 73: 1508-1510.

Govindjee, S., Sackman, J. L. (1999): On the use of continuum mechanics to estimate the properties of nanotubes. *Solid state comm.*. 110: 227-230.

Hernandez, E., Goze, C., Bernier, P., Rubio, A. (1998): Elastic properties of C A and B_x C_y N_z composite nanotubes. *Phys Rev Lett.*. 80:4502-45025.

Han, X., Liu, G. R., Li G. Y., (2004); Transient Response in Cross-Ply Laminated Cylinders and Its Application to Reconstruction of Elastic Constants, *CMC: Computers, Materials & Continua*. 1 (1): 39-49.

Li, C. Y., Chou, T. W. (2003): Multiscale Modeling of carbon nanotube reinforced polymer composites. *Journal of Nanoscience and Nanotechnology*. 3 (5): 423-430.

Liu, G. R. , Tani, J., Ohyoshi, T. and Watanabe, K. (1991): Transient waves in anisotropic laminated plates, Part 1: Theory, Part 2: Application, *ASME Journal of Vibration and Acoustics, U. S. A.*. Vol. 113: 235-239.

Liu, G. R., Xi, Z. C. (2001): Elastic waves in anisotropic laminates. CRC press.

Liu, Z., Zheng, Q. S. (2002): A few problems on mechanics of the carbon nanotube, Tsinghua university, China, Ph. D thesis.

Lysmer, J. (1970): Lumped mass method for Rayleigh waves, *Bull. Seismological Soc.Am.*. 60(1), 89-104.

Qian, D., Wagner, G. J., Liu, W. K., Yu, M. F., Ruoff, R. S. (2002): Mechanics of carbon nanotubes, *Applied Mechanics Review*. 55(5):495-533.

Poncharal, P., Wang, Z., Ugarte, D. de., Heer, W. (1999): Electrostatic deflections and electromechanical resonances of carbon nanotubes. *Science*. 283: 1513-1516.

Popov, V., Doren, V. (2003); Elastic properties of single-walled carbon nanotubes. *Phys. Rev. B.*. 61: 3078-3084.

Parnes, R.,Chiskis, A. (2002): Buckling of nanofiber reinforced composites: a re-examination of elastic buckling. *Journal of the Mechanics and Physics of Solids*. 50: 855-879.

Salvetat, J. P., Briggs, G. A. D., Bonard, J. M., Bacsa, R. R., Kulik, A. J., Stockli. T. et al. (1999): Elastic and shear moduli of single-walled carbon nanotubes. *Phys Rev Lett.*. 82:944-947.

Treacy, M., Ebbesen, T., Gibson, J. (1996): Exceptionally high Young's modulus observed for individual carbon nanotubes. *Nature*. 381: 678-689.

Wang, Q., Varadan, V. K. (2006): Wave characteristics of carbon nanotubes. *International Journal of Solids and Structures*. 43(2): 254-265.

Xi, Z. C., Liu, G. R., Lam, K. Y. and Shang, H. M. (2000): Dispersion and characteristic surfaces of waves in laminated composite circular cylindrical shells, *Journal of the Acoustical Society of America*. Vol.108(5). 2179-2186.

Xie, G. Q. and Long, S. Y. (2006): Elastic vibration behaviors of carbon nanotubes based on micropolar mechanics. *CMC: Computers, Materials & Continua*. 4(1):11-22.

Yoon, J., Ru, C., Mioduchowski, A. (2002): Non-coaxial resonance of an isolated multi-wall carbon nanotube, *Phys. Rev B.*. 66: 233402-233407.

Yoon, J., Ru, C., Mioduchowski, A. (2003a): Sound wave propagation in multiwall carbon nanotubes. *J. Appl. Phys.*. 93(8): 4801-4806.

Yoon, J., Ru, C., Mioduchowski, A. (2003b): Vibration of embedded multiwall carbon nanotubes composites. *Sci.Technol.*. 63: 1533-1542.

Zhang,Y. Q., Liu,G. R., Han, X. (2005): Transverse vibrations of double-walled carbon nanotubes under compressive axial load. *Physics Letters*. A. 340: 258-266.